Atypical Neurofibromas in Neurofibromatosis Type 1 are Premalignant Tumors

Eline Beert,[1] Hilde Brems,[1] Bruno Daniëls,[2] Ivo De Wever,[3] Frank Van Calenbergh,[4] Joseph Schoenaers,[5] Maria Debiec-Rychter,[1] Olivier Gevaert,[6] Thomas De Raedt,[7] Annick Van Den Bruel,[8] Thomy de Ravel,[1] Karen Cichowski,[7] Lan Kluwe,[9,10] Victor Mautner,[9] Raf Sciot,[11] and Eric Legius[1]*

[1]Department of Human Genetics, Catholic University Leuven, Leuven, Belgium
[2]Department of Biosystems, Catholic University Leuven, Leuven, Belgium
[3]Department of Surgical Oncology, University Hospitals Leuven, Leuven, Belgium
[4]Department of Neurosurgery, University Hospitals Leuven, Leuven, Belgium
[5]Department of Craniomaxillofacial Surgery, University Hospitals Leuven, Leuven, Belgium
[6]Department of Radiology, Stanford University School of Medicine, Stanford, CA
[7]Genetics Division, Department of Medicine, Harvard Medical School, Boston, MA
[8]Department of Internal Medicine, A Z Sint-Jan, Bruges, Belgium
[9]Department of Maxillofacial Surgery, University Hospital Eppendorf, Hamburg, Germany
[10]German Cancer Research Center, Heidelberg, Germany
[11]Department of Pathology, Catholic University Leuven, Leuven, Belgium

Benign peripheral nerve sheath tumors (PNSTs) are a characteristic feature of neurofibromatosis type 1 (NF1) patients. NF1 individuals have an 8–13% lifetime risk of developing a malignant PNST (MPNST). Atypical neurofibromas are symptomatic, hypercellular PNSTs, composed of cells with hyperchromatic nuclei in the absence of mitoses. Little is known about the origin and nature of atypical neurofibromas in NF1 patients. In this study, we classified the atypical neurofibromas in the spectrum of NF1-associated PNSTs by analyzing 65 tumor samples from 48 NF1 patients. We compared tumor-specific chromosomal copy number alterations between benign neurofibromas, atypical neurofibromas, and MPNSTs (low-, intermediate-, and high-grade) by karyotyping and microarray-based comparative genome hybridization (aCGH). In 15 benign neurofibromas (4 subcutaneous and 11 plexiform), no copy number alterations were found, except a single event in a plexiform neurofibroma. One highly significant recurrent aberration (15/16) was identified in the atypical neurofibromas, namely a deletion with a minimal overlapping region (MOR) in chromosome band 9p21.3, including *CDKN2A* and *CDKN2B*. Copy number loss of the *CDKN2A/B* gene locus was one of the most common events in the group of MPNSTs, with deletions in low-, intermediate-, and high-grade MPNSTs. In one tumor, we observed a clear transition from a benign-atypical neurofibroma toward an intermediate-grade MPNST, confirmed by both histopathology and aCGH analysis. These data support the hypothesis that atypical neurofibromas are premalignant tumors, with the *CDKN2A/B* deletion as the first step in the progression toward MPNST.

INTRODUCTION

Neurofibromatosis type I (NF1) is a common, autosomal dominant disorder caused by heterozygous inactivating mutations in the *NF1* tumor suppressor gene (chromosome band 17q11.2) (Cawthon et al., 1990; Viskochil et al., 1990; Wallace et al., 1990). This gene encodes neurofibromin, a negative regulator of the "rat sarcoma viral oncogene homologue" (RAS) (Martin et al., 1990). The main clinical characteristics are café-au-lait maculae, skin fold freckling, Lisch nodules, and neurofibromas. Other features include optic pathway gliomas, specific osseous lesions, and learning disabilities.

Neurofibromas are benign tumors of the peripheral nerve sheath. Different types can be recognized: cutaneous, subcutaneous (s.c.), and plexiform neurofibromas. Each NF1 patient has an estimated 8–13% cumulative risk of developing a malignant peripheral nerve sheath tumor (MPNST) (Evans et al., 2002). This risk is even two or three times higher in patients with an *NF1* microdeletion compared with patients with an intragenic *NF1* mutation (De Raedt et al., 2003). MPNSTs are often difficult to diagnose in the early phase; they metastasize widely and are associated with a poor

Additional Supporting Information may be found in the online version of this article.

*Correspondence to: Dr. Eric Legius, Department of Human Genetics, Catholic University Leuven, Herestraat 49, B-3000 Leuven, Belgium. E-mail: eric.legius@uzleuven.be

Received 13 April 2011; Accepted 21 July 2011

DOI 10.1002/gcc.20921

Published online 24 August 2011 in Wiley Online Library (wileyonlinelibrary.com).

prognosis. The 5-year survival rate is <25% (Evans et al., 2002).

Neurofibroma-derived Schwann cells, harboring both a germline and somatic mutation in the *NF1* gene, are believed to be the primary neoplastic cells in neurofibromas (Serra et al., 2000). Biallelic *NF1* inactivation also occurs in MPNSTs (Legius et al., 1993), but it is not sufficient for MPNST formation. Additional alterations in tumor suppressor genes *TP53* and *CDKN2A* have been identified in MPNSTs. The "tumor protein 53" (*TP53*) gene (chromosome band 17p13.1) encodes p53 and is involved in cell cycle control, apoptosis, and DNA damage response. *TP53* deletion/mutation is one of the most common abnormalities found in MPNSTs (Menon et al., 1990; Legius et al., 1994; Birindelli et al., 2001). The "cyclin-dependent kinase inhibitor 2A" (*CDKN2A*) gene (chromosome band 9p21.3) encodes both $p16^{INK4A}$, a negative regulator of the cell cycle, and $p14^{ARF}$, a protein that promotes stabilization of p53 through binding with "mouse double minute 2 homologue" (MDM2). Homozygous *CDKN2A* deletions are found in 50% of MPNSTs (Kourea et al., 1999; Nielsen et al., 1999). None of the abnormalities described earlier are present in neurofibromas.

In addition to tumor suppressor alterations, there is also evidence for aberrant signaling through growth factors and their receptors in MPNST pathogenesis. Gene amplification of *EGFR*, *ERBB2*, *KIT*, *HGF*, and *MET* and amplifications/mutations in *PDGFRA* have been detected in MPNSTs (Perry et al., 2002; Holtkamp et al., 2006; Storlazzi et al., 2006; Mantripragada et al., 2008). Like most sarcomas, MPNSTs have a complex and variable karyotype with multiple chromosomal gains and losses (Glover et al., 1991). Recurrent copy number gains are found on chromosomes 7, 8q, 15q, and 17q and losses on 1p, 9p, 11, 12p, 14q, 17q, 18, 22q, X, and Y (Mertens et al., 1995, 2000; Lothe et al., 1996; Schmidt et al., 2000, 2001; Storlazzi et al., 2006; Mantripragada et al., 2009).

The spectrum of PNSTs ranges from benign to high-grade malignant. It is presently unknown where atypical neurofibromas fit into this system. On pathological examination, no mitoses are detected, similarly to the typical benign neurofibromas. However, atypical neurofibromas show a more variable cellularity and have cells with enlarged, hyperchromatic nuclei. Clinically, atypical neurofibromas might cause pain and are frequently (slow) growing tumors with an increased glucose uptake on fluorine-18-labeled fluorodeoxyglucose (^{18}F-FDG)-PET scan (Ferner et al., 2008). These tumors may be a transition state between neurofibromas and MPNSTs (Nielsen et al., 1999; Brems et al., 2009).

We performed karyotyping and high-resolution Agilent 244K microarray-based comparative genome hybridization (aCGH) on 16 histopathologically confirmed, atypical neurofibromas. To situate the atypical neurofibroma in the malignant transformation process, 15 benign neurofibromas and 34 MPNSTs were also analyzed using the same methods. Because of their potential role in MPNST development, *TP53* and *CDKN2A* were sequenced for mutations.

MATERIALS AND METHODS

Tumor Material

The tumor samples were collected from the University Hospitals of Leuven, Eppendorf (Hamburg), AZ Sint-Jan (Bruges), and the Harvard Medical School (Boston). Part of the tumor was snap frozen and used for DNA isolation with phenol/chloroform. The other part was dissociated and used for cell culture as described earlier (Serra et al., 2000). We established primary cell cultures from six high-grade MPNSTs (HM1–3, HM9, and HM22–23). Tumor cells from HM1–2, HM9, and HM22 were cultured under specific $NF1^{-/-}$ Schwann cell conditions. Cells from HM3 and HM23 were cultured in a general tumor medium, as they did not grow in Schwann cell medium. The presence of MPNST tumor cells was confirmed by karyotyping at the end of the culture.

The tumor samples were removed from 48 patients, fulfilling two or more NF1 diagnostic criteria, established at the NIH Consensus Development Conference in 1987. Ten patients carried an *NF1* microdeletion, of which nine patients were type I (De Raedt et al., 2004) and one patient was type II (Kehrer-Sawatzki et al., 2004). Patient blood DNA was available from 24 of 48 patients. If not available, blood DNA from a healthy male or female individual was used as a gender-matched control in aCGH experiments.

The current research protocol was approved by the local ethical committee of the University Hospitals Leuven (S52563).

Histopathology

Depending on their histopathological features (Scheithauer et al., 1999), the 65 tumor samples

were subdivided in six distinct categories: s.c. (4), plexiform (11), atypical neurofibromas (16), low- (2), intermediate- (2), and high-grade MPNSTs (30). The histological grading of MPNSTs was based on the "Fédération Nationale des Centres de Lutte Contre le Cancer" grading system (Guillou et al., 1997).

Cytogenetic Analysis

Conventional cytogenetic analysis was performed on G-banded metaphases, obtained after a short-term *NF1*$^{-/-}$ Schwann cell culture, according to standard procedures (Polito et al., 2003). If there were sufficient mitoses, at least 15 metaphases were analyzed. Karyotypes were described using the "International System for Human Cytogenetic Nomenclature" (ISCN 2009) criteria.

Mutation Analysis

TP53 and *CDKN2A* mutation analysis was performed on tumor and patient blood DNA, if available. Exons 2–9 of *TP53* and all *CDKN2A* exons were PCR amplified and bidirectionally sequenced on the ABI 3100 using the ABI BigDye Terminator 3.1 Sequencing kit (Applied Biosystems, Carlsbad, CA).

aCGH

Agilent 244K aCGH

All samples were analyzed using the 244K high-resolution oligonucleotide microarray from Agilent Technologies (Diegem, Belgium). Digestion, labeling, and hybridization of tumor and patient or gender-matched blood DNA were performed according to the protocol of the manufacturer ("Agilent Oligonucleotide Array-based CGH for Genomic DNA Analysis," Enzymatic Labeling for Blood, Cells, or Tissues (with High Throughput option) v6.2.1, February 2010).

The level of copy number losses and gains was checked visually in the individual profiles. Chromosomal regions with a minimum average $\log_2$ratio of 0.15 were considered as gains and of −0.15 as losses. A loss was called homozygous when the $\log_2$ratio was lower than −1, and a gain was called an amplification when the $\log_2$ratio was higher than 0.58. When gender-matched control DNA was used from an unrelated individual (patient blood DNA was not available), somatic copy number variations were excluded if they occurred in known copy number variable regions indicated by the Genomic Workbench Software.

Statistical Analysis of Recurrent DNA Copy Number Gains and Losses

The Agilent 244K aCGH data were used as obtained from the Agilent Feature Extraction software. The datasets of 16 atypical neurofibromas and 23 independent primary high-grade MPNSTs were both analyzed with the KCsmart software for statistically significant recurrent copy number gains and losses (Klijn et al., 2008). The datasets of the benign neurofibromas, low-, and intermediate-grade MPNSTs were not analyzed for recurrent chromosomal aberrations because of the small number of alterations or samples in the dataset.

We removed all clones where at least one $\log_2$-ratio was missing. A KCsmart 1000 permutation analysis was performed to create a null distribution. Peaks were detected at $P < 0.05$ (Bonferroni corrected for multiple testing), for different kernel widths between 5 Mb and 100 kb.

RESULTS

Clinical Data

The patients' gender, presence/type of *NF1* microdeletion, age at surgery (years), and information on the tumors (type, location, and material) are summarized in Table 1. We evaluated 65 tumor samples (59 snap frozen and six cell lines) originating from 62 different PNSTs. At the time of surgery, the patients' age ranged from 9 to 63 years. From the 58 tumors with known location, 26 were localized in the trunk, 25 in the extremities, and 7 in the head–neck region.

Cytogenetic Analysis

An overview of all karyotypes can be found in Supporting Information Table 1. Karyotypes were available for 10/15 benign neurofibromas (two s.c. and eight plexiform). No clonal cytogenetic aberrations were observed in the majority of tumors. In one plexiform neurofibroma (PN10), almost all cells showed a deletion at chromosome band 7p15, which was later confirmed by Agilent 244K aCGH analysis. We observed one cell in a tetraploid state in PN10.

In 11 out of 14 karyotyped atypical neurofibromas, chromosome 9 was involved in the chromosomal rearrangements in 13–100% of analyzed

TABLE 1. Summary of Clinical Data

Patient	Gender	Presence/ type *NF1* microdeletion	Age at surgery (years)	Neurofibroma			MPNST			Tumor location	Tumor material
				Benign			Grade				
				SCN	PN	A	LM	IM	HM		
1	F	–	29						HM1	Back	Cell line
2	F	–	18						HM2	Femur	Cell line
3	F	Type I	17						HM3	Forearm left	Cell line
4	F	–	18		PN1					Wrist/hand	Tissue
5	M	–	34					IM1		Thorax right	Sections
6	M	–	31						HM4	Forearm right	Tissue
7	M	Type I	58						HM5	Pancreas	Tissue
8	F	–	60			A1				Mediastinum	Tissue
9	M	–	9		PN2					Face	Tissue
10	M	–	41						HM6	Lower leg	Sections
11	M	–	18		PN3					Femur left	Sections
12	F	–	19		PN4					Ankle	Tissue
13	M	Type I	18		PN5					Leg	Tissue
14	M	Type I	36						HM7	Neck	Tissue
15	F	–	55		PN6					Lower leg	Tissue
16	M	–	30		PN7					Femur left	Tissue
17	M	Type I	24						HM8	Femur left	Sections
			30		PN8	A2				Thorax left	Tissue
18	M	–	42		PN9					Parasternal right	Tissue
19	F	–	32			A3				Forearm left	Sections
20	M	Type I	22						HM9	Upperarm left[a]	Cell line
			28				LM1			Shoulder left	Tissue
			28			A4				Paravertebral	Sections
21	F	–	15			A5				Leg	Sections
22	M	–	30			A6				Retroperitoneal right	Tissue
23	F	–	18			A7		IM2		Thorax top right	Tissue
24	M	Type I	21						HM10	Back	Sections
			22						HM11	Lung metastasis	Tissue
25	F	–	27	SCN1						Lower leg left	Tissue
26	F	Type I	27						HM12	Left lower leg	Sections
27	F	–	38			A8				Left N. femoralis	Sections
28	F	–	21	SCN2						Leg	Tissue
29	M	–	44			A9				N. ischiadicus right	Sections
			44						HM13	N. ischiadicus right	Tissue
			44						HM14	Paravertebral D12	Tissue
			44	SCN3						Back	Tissue
30	F	–	26						HM15	Pelvis	Sections
			29						HM16	Pelvis (recurrence)	Sections
31	F	–	23				LM2			Right upper arm	Sections
			25			A10				Occipital region	Sections
			26			A11				Plexus brachialis left	Tissue
32	F	–	27		PN10					Ankle	Tissue
33	M	–	31		PN11				HM17	Abdomen	Tissue
			31						HM18	Abdomen (recurrence)	Tissue
34	F	–	14	SCN4						Popliteal area right	Tissue
35	F	–	u			A12				u	Tissue
36	F	–	58			A13				Neck left	Sections
37	F	–	63						HM19	u	Tissue
38	M	Type I	23						HM20	Bowel	Tissue
			26						HM21	Bowel (recurrence)	Tissue
39	M	–	21						HM22	u	Cell line
40	F	–	33						HM23	Ischiorectal fossa left	Cell line
41	M	Type II	17						HM24	u	Tissue
42	F	–	35			A14				Mediastinum	Tissue
43	M	–	26			A15				N. vagus right, neck	Sections
44	F	–	28			A16				Thoraco-lumbal left, back	Sections

(Continued)

TABLE 1. Summary of Clinical Data (Continued)

Patient	Gender	Presence/ type *NF1* microdeletion	Age at surgery (years)	Neurofibroma			MPNST			Tumor location	Tumor material
				Benign			Grade				
				SCN	PN	A	LM	IM	HM		
45	F	–	24						HM25	C1 right[b]	Sections
46	F	–	51						HM26	Back	Tissue
			51						HM27	Throat (recurrence)	Tissue
47	M	–	u						HM28	Groin	Tissue
			u						HM29	Lung metastasis	Tissue
48	F	–	40						HM30	Thorax	Tissue

[a]Recurrence after chemotherapy.
[b]After radiotherapy as a child for a brain tumor.
Note: F: female; M: male; –: not present; u: unknown; SCN: subcutaneous neurofibroma; PN: plexiform neurofibroma; A: atypical neurofibroma; LM: low-grade MPNST; IM: intermediate-grade MPNST; HM: high-grade MPNST.

cells. Besides chromosome 9, aberrations on other chromosomes were also frequently observed. Nine atypical neurofibromas showed a triploid or tetraploid state in 10–67% of analyzed cells.

According to their karyotypes, the two low-grade MPNSTs differed from each other. LM1 had multiple alterations affecting chromosomes 1, 2, 6, 8, 10, 13, and 21. One of the analyzed cells of LM1 showed a tetraploid state. In LM2, there were deletions on the short arm of chromosome 9 in 16 and an isochromosome 7 in 2 out of 18 analyzed cells.

One intermediate and 11 investigated high-grade MPNSTs showed multiple complex chromosomal aberrations in 20–100% of analyzed cells. Polyploidy ($\geq 3n$) was observed in the intermediate-grade MPNST and in 5 out of 11 high-grade MPNSTs.

CDKN2A and *TP53* Mutation Analysis

CDKN2A and *TP53* were sequenced for mutations in tumor and patient blood DNA, if available. No mutations were found in 15 benign and 16 atypical neurofibromas. The *CDKN2A* mutation c.203dupC, detected in LM1, was located in exon 2 (codon 68), resulting in a frameshift and a premature stop codon (p.A68AfsX119). The relative height of the mutation peak is 40% of the normal peak, suggesting a heterozygous mutation in 80% of the cells. In three out of six high-grade MPNST cell lines (HM2, HM3 and HM23), a heterozygous *TP53* point mutation was present in all cells. Mutation c.329G>C (p.R110P) (HM2) and c.535C>T (p.H179Y) (HM23) were situated in the DNA binding domain, a highly conserved region in the *TP53* gene. Mutation c.96 + 1G>A was identified as a splice site mutation in HM3. There was no frozen tumor tissue left to confirm the mutation found in the MPNST cell lines.

Agilent 244K aCGH Analysis

Benign neurofibromas

Four s.c. and 11 plexiform neurofibromas were screened for genome wide copy number alterations using the Agilent 244K oligonucleotide microarray. In one plexiform neurofibroma (PN10), we identified two deletions ($\log_2$ratio = −0.5) on the short arm of chromosome 7, namely a 1.83Mb (p21.1-p15.3) and a 31.97Mb (p15.3-p11.2) deletion. None of these regions were part of the recurrent copy number losses in atypical neurofibromas or MPNSTs.

Atypical neurofibromas

In 15 of 16 atypical neurofibromas, we detected deletions on the short arm of chromosome 9, resulting in several minimal overlapping regions (MORs) (Table 2), with 9p21.3 being the most commonly deleted region (Fig. 1). The length of this deletion varied from 0.22 to 39.60 Mb, with a minimum overlap of 0.16 Mb localized at 21.95–22.11 Mb (Human Genome Build NCBI36), including *CDKN2A* and *CDKN2B*. Because of tumor heterogeneity, only in one atypical neurofibroma (A2), the 9p loss could be considered as a homozygous deletion ($\log_2$ratio = −2.5) in almost all cells. For five samples (A7, A9, A11, A14, and A16), the $\log_2$ratio of the 9p21.3 deletion was more negative than the other deletions on 9p, suggesting a homozygous deletion at 9p21.3. Apart from the 9p21.3 deletion, there were seven additional MORs at 9p, including the *SMARCA2*, *RFX3*, *GLIS3*, *PTPRD*, and *LRRN6C* genes (Table 2). Additional copy number changes were observed in 13 atypical neurofibromas, but these alterations were far less frequent and occurred in a lower percentage of cells, compared with the 9p21.3 deletion (Supporting Information Table 2).

TABLE 2. MORs on Chromosome 9p in Atypical Neurofibromas and High-Grade MPNSTs

Minimal overlapping region 9p	Chromosomal band	Atypical neurofibromas			High-grade MPNSTs			Genes
		Start (Mb)	Stop (Mb)	Frequency	Start (Mb)	Stop (Mb)	Frequency	
1	9p24.3	0.99	1.89	6/16 (38%)	1.69	1.86	11/23 (48%)	/
2	9p24.3-p24.2	1.92	2.22	6/16 (38%)	1.99	2.16	11/23 (48%)	*SMARCA2*
3	9p24.2	2.87	4.44	6/16 (38%)	2.78	3.86	11/23 (48%)	*RFX3, GLIS3*
4	9p24.1-p23	8.50	11.33	6/16 (38%)	8.50	8.81	11/23 (48%)	*PTPRD*
5	9p22.3	15.69	15.96	5/16 (31%)	/	/	/	/
6	9p21.3	21.95	22.11	15/16 (94%)	21.95	22.01	16/23 (70%)	*CDKN2A, CDKN2B*
7	9p21.1	28.17	28.20	6/16 (38%)	/	/	/	/
8	9p21.1	28.36	29.05	6/16 (38%)	28.37	29.05	14/23 (61%)	*LRRN6C*

Note: the start and stop position of the MORs was based on Human Genome Build NCBI36.

The alterations found in atypical neurofibromas were frequently detected in high-grade MPNSTs.

MPNSTs

Both low-grade MPNSTs showed a deletion of the *CDKN2A/B* gene region, heterozygous in LM1, and homozygous in LM2. A complex aCGH profile with multiple gains and losses, but different from each other, was detected in the intermediate MPNSTs. IM1 had many copy number changes, more gains than losses, in almost all cells, but no deletion on the short arm of chromosome 9. In IM2, the number of alterations was smaller than in IM1 and occurred in a lower percentage of cells (20–30%). This might reflect the admixture with normal and atypical cells, since sample IM2 and A7 were obtained from the same tumor, as the inner and outer part, respectively (Fig. 2A). By sampling, we were not able to clearly separate the neurofibroma from the atypical neurofibroma part, but based on histopathology we could. The alterations found in IM2 were those present in A7 but with additional losses on chromosome 1p, 10, 11, and 21 (Fig. 2B). One of the observed tumor specific copy number losses was a type II *NF1* microdeletion in A7 and IM2, presenting the somatic *NF1* mutation in this tumor (Fig. 2C).

An overview of all alterations in low- and intermediate-grade MPNSTs is shown in Supporting Information Table 2.

In the high-grade MPNST group, 23 independent primary tumors were analyzed. Seven other samples came from metastases of primary tumors (HM11 and HM29), recurrences after surgery (HM16, HM18, HM21, and HM27), or recurrences after surgery and chemotherapy (HM9). These latter tumors were analyzed as a separate group and were not part of the group of 23 independent primary tumors. Supporting Information Table 3 gives a detailed overview of all of the statistically significant recurrent copy number altered regions (visualized in Fig. 3, using the KCsmart analysis tool), MORs, (candidate) cancer genes, and microRNAs, in the 23 independent primary high-grade MPNSTs. Sixteen of 23 high-grade MPNSTs (70%) showed copy number loss of the *CDKN2A/B* gene locus, of which 12 were considered homozygous. Loss of *TP53* was observed in 12 high-grade MPNSTs. In addition to *CDKN2A* and *TP53*, other genes were frequently involved in recurrent chromosomal rearrangements (Fig. 3 and Supporting Information Table 3). Gain of the *PDGFRA/KIT* (4q12), the *TWIST1* (7p21.1), the *EGFR* (7p11.2), the *MET* (7q31.2), and the *MYC* region (8q24.21) was observed in 13, 18, 17, 15, and 16/23 high-grade MPNSTs, respectively. Of note is the copy number gain of *CCND2* (12p13.32) and *MDM2* (12q15) in 11 and 9 high-grade MPNSTs, respectively. Additionally, large segments of chromosome arms 14q, 15q, 17q, 20q, and 21q were frequently duplicated or amplified.

Deletions on the short arm of chromosome 1 were identified in 17 of 23 high-grade MPNSTs. HM23 had a deletion of the total 1p-arm, with defined homozygous deletions of *PRDM2*, *CDKN2C*, *RNF11*, *EPS15*, *NFIA*, *PGM1*, *ROR1*, *UBE2U*, *CACHD1*, *RAVER2*, and *JAK1*. A deletion of hsa-mir-101-1, a cancer-related microRNA located at 1p31.3, was found in 15 high-grade MPNSTs. Parts of chromosome arm 3q were lost in 16 high-grade MPNSTs, with focal deletions of genes *LSAMP* (3q13.31), *EPHB1* (3q22.2), and *STAG1* (3q22.3). Remarkable was the recurrent copy number loss on chromosome arm 4q, including *SMARCD1* (4q22.3) and *SPRY1* (4q28.1), in 9

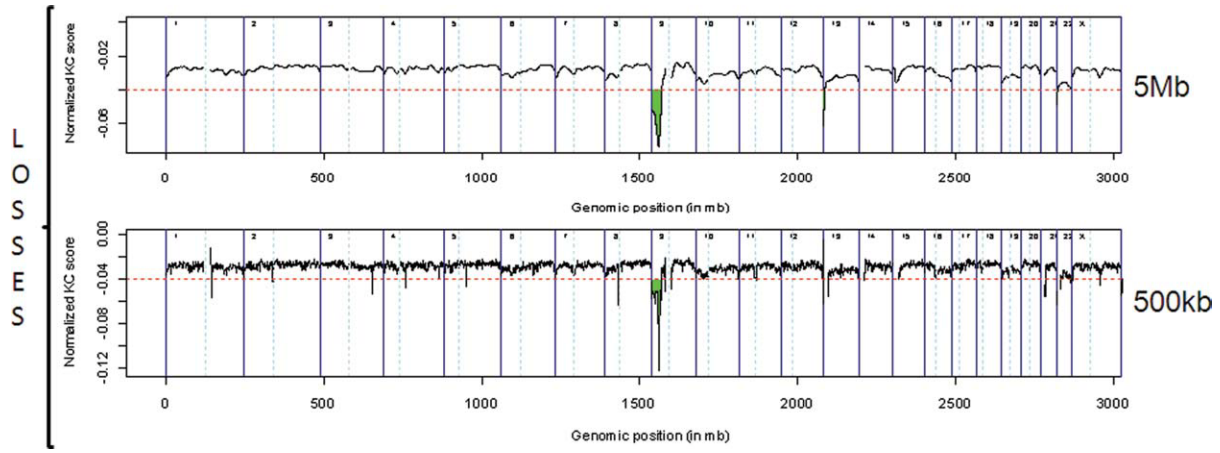

Figure 1. Recurrent copy number loss profile of 16 atypical neurofibromas. The figure represents the profile of copy number losses using kernel width 5 Mb (upper part) and 500 kb (lower part), with on the *X*-axis the genomic position in Mb and on the *Y*-axis the normalized KC-score, calculated by the KCsmart program. The blue continuous lines mark out the different chromosomes, and the blue dashed lines represent the position of the centromeres. The 5% significance level is marked with a red dashed line. Regions with a normalized KC-score exceeding the significance level are labeled in green. The peak at chromosome 9p was considered as the only significantly recurrent copy number loss in 16 atypical neurofibromas. The other visible peaks were localized at copy number variable or pericentromeric heterochromatin regions and were not part of the significantly recurrent deletions.

and 10 tumors, respectively. In 14 high-grade MPNSTs, the *PTEN* gene (10q23.31) was deleted. (Partial) loss of chromosome arms 11p and 11q was observed in 19 and 20 high-grade MPNSTs, respectively. The *CDKN1C* gene (11p15.4) was lost in 14 high-grade tumors. The region with the highest deletion frequency (18/23) on chromosome 11 (11q22.3-q23.1) included the genes *ATM*, *DDX10*, and cancer-related microRNAs hsa-mir-34b and c. The *RB1* (13q14.2), *SPRY2* (13q31.1), and *SUZ12* gene (17q11.2) was deleted in 12, 14, and 17 high-grade MPNSTs, respectively. The long arm of chromosome 22 or parts of it were frequently lost, including several tumor suppressor genes such as *CHEK2* (22q12.1) and *NF2* (22q12.2), which were deleted in 13 high-grade MPNSTs.

When analyzing the metastases (HM11 and HM29) or recurrences (HM9, HM16, HM18, HM21, and HM27), no or minor recurrent copy number alterations other than those already observed in the group of the independent primary tumors were identified.

DISCUSSION

This is the first report where large numbers of histopathologically confirmed benign and atypical neurofibromas and MPNSTs (low-, intermediate-, and high-grade) are evaluated by conventional cytogenetics, high-resolution Agilent 244K aCGH and *CDKN2A*/*TP53* mutation analysis.

Biallelic inactivation of *NF1* and subsequent loss of neurofibromin in Schwann cells leads to prolonged activation of RAS and increased cell proliferation. Although this is sufficient for neurofibroma formation, further genetic events are necessary in the progression pathway toward malignancy.

In 15 of the 16 atypical neurofibromas, a deletion at 9p21.3 was observed. In six cases, this 9p21.3 deletion was interpreted as homozygous as a lower $\log_2$ratio was found in this region compared with the nearby deleted loci on chromosome arm 9p. Two genes are located in the MOR, namely *CDKN2A* and *CDKN2B*. The *CDKN2A* locus encodes $p16^{INK4A}$ and $p14^{ARF}$, which are negative regulators of the cell cycle through interaction with RB1 and p53. The "cyclin-dependent kinase inhibitor 2B" (*CDKN2B*) gene encodes $p15^{INK4B}$, which controls the cell cycle G1 progression by interacting with CDK4 and CDK6. This gene is located adjacent to the *CDKN2A* gene locus and is often codeleted with *CDKN2A* in MPNSTs (Perrone et al., 2003; Mantripragada et al., 2009). Deletion of *CDKN2A*/*B* was identified in 70% of independent primary high-grade MPNSTs. Previous reports on the involvement of *CDKN2A* in NF1-related MPNSTs have revealed alterations in 40–60% of cases. In contrast with MPNSTs, studies on neurofibromas did not reveal *CDKN2A* abnormalities (Kourea et al., 1999; Nielsen et al., 1999; Mantripragada et al., 2008, 2009).

Several other genes, located on chromosome arm 9p, were frequently involved in atypical neurofibromas and high-grade MPNSTs. Few of

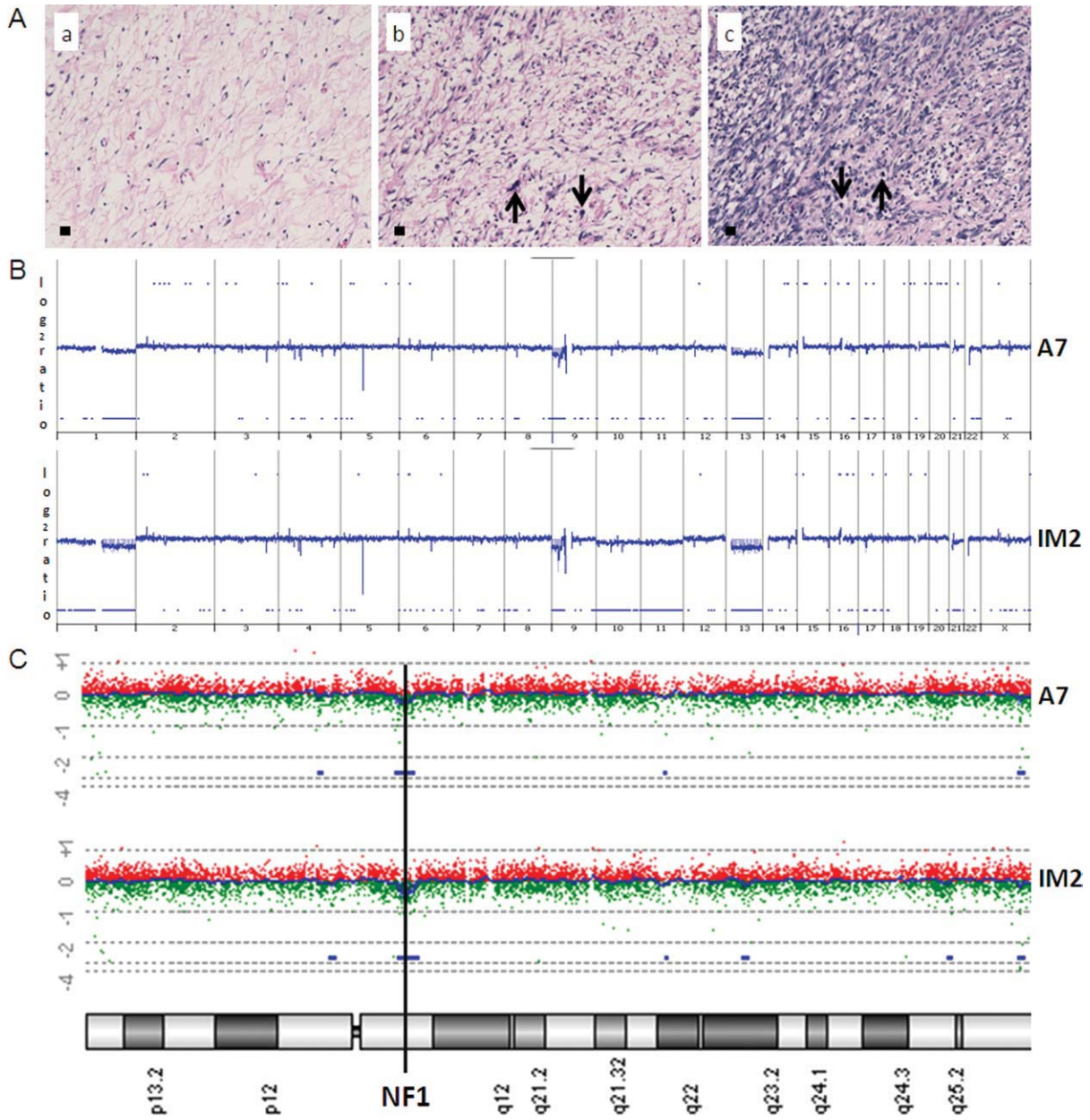

Figure 2. Histopathology and aCGH data on the PNST of Patient 23. Panel A: histopathology: (a) outer part: benign neurofibroma: note the low cellularity and the typical wavy nuclei and cell processes, as well as the loose collagenous background. (b) Middle part: atypical neurofibroma: lesion with a variable and locally increased cellularity with the characteristic presence of enlarged hyperchromatic nuclei (black arrows), in the absence of mitotic figures. (c) Inner part: intermediate grade MPNST: lesion with long hypercellular fascicles of atypical spindle cells with numerous mitotic figures (black arrows); hematoxylin & eosin stain; Leica DMLB microscope; black bars = 20 microns. Panel B: aCGH: whole genome view of A7 (top) and IM2 (bottom). Note that the copy number alterations in A7 are also part of those seen in IM2. *X*-axis: genomic location per chromosome; *Y*-axis: $\log_2$ratio; blue line: moving average of $\log_2$ratio. Panel C: aCGH: detailed view on chromosome 17 in A7 (top) and IM2 (bottom). Note the presence of the same type II microdeletion as the somatic *NF1* mutation. *X*-axis: genomic location on chromosome 17; *Y*-axis: $\log_2$ratio; red dots ($\log_2$ratio > 0), green dots ($\log_2$ratio < 0), blue line (moving average of $\log_2$ratio).

these genes have previously been linked to cancer. "SWI/SNF-related matrix-associated actin-dependent regulator of chromatin subfamily a member 2" (*SMARCA2*), lost in six atypical neurofibromas and 11 high-grade MPNSTs, encodes the protein "Brahma" (BRM) that functions as the ATPase subunit in the ATP-dependent SWI/SNF chromatin remodeling complex. BRM is a

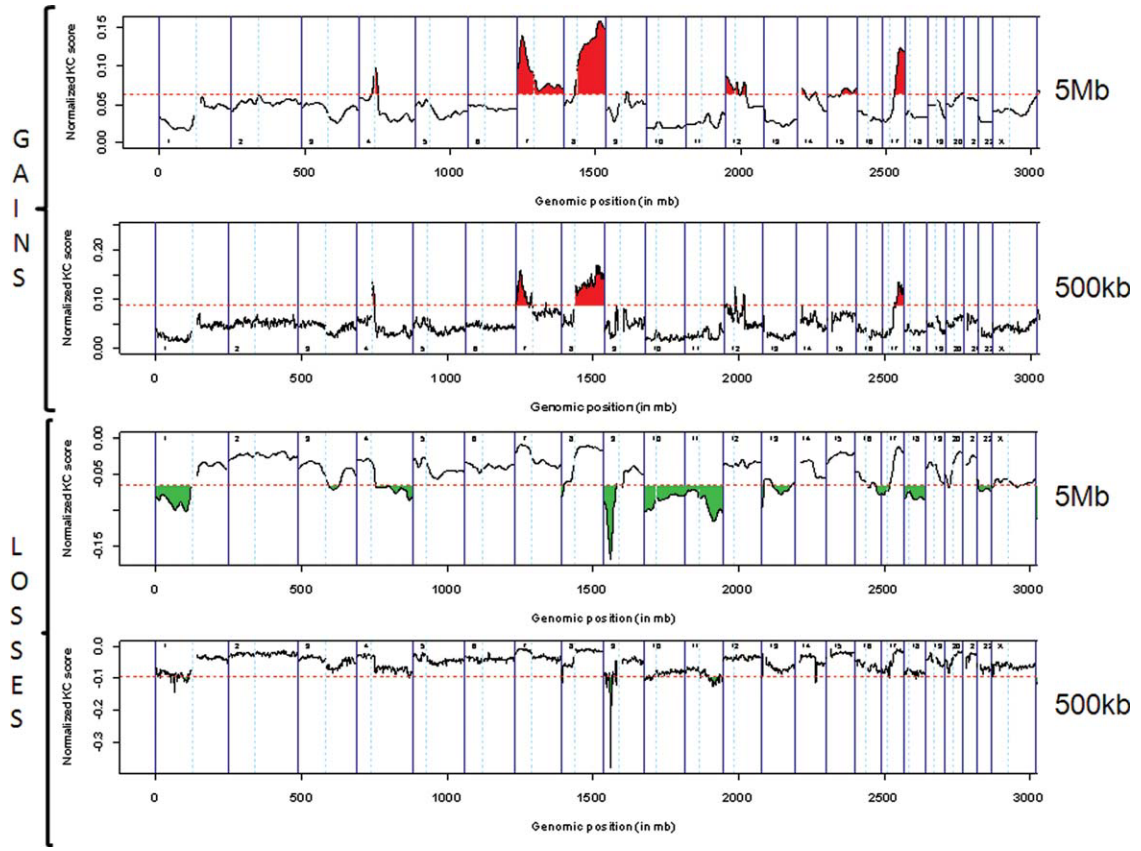

Figure 3. Recurrent copy number alterations profile of 23 independent primary high-grade MPNSTs. The upper part of the figure represents the profile of the copy number gains using kernel widths 5 Mb and 500 kb, with on the *X*-axis the genomic position in Mb and on the *Y*-axis the normalized KC-score, calculated by the KCsmart program. The blue continuous lines mark out the different chromosomes, and the blue dashed lines represent the position of the centromeres. The 5% significance level is marked with the red dashed line. In the lower part of the figure, the copy number losses are plotted using kernel widths of 5 Mb and 500 kb. Regions with a normalized KC-score exceeding the significance level are labeled in red or green for gains or losses, respectively. Statistically recurrent copy number losses were found at chromosome 1, 3, 4, 8, 9, 10, 11, 13, 14, 16, 17, 18, 20, 22, and X and gains at chromosome 4, 7, 8, 12, 14, 15, 17, 20, and 21.

negative regulator of cell cycle progression in vitro as it induces cell cycle arrest by cooperating with RB1 in repressing E2F1 (Trouche et al., 1997). The "protein tyrosine phosphatase receptor type D" (*PTPRD*) gene, also lost in six atypical neurofibromas and 11 high-grade MPNSTs, encodes a transmembrane protein with a cytoplasmic tyrosine phosphatase domain. *PTPRD* is a candidate tumor suppressor gene as it is inactivated in glioblastoma and other human cancers (Veeriah et al., 2009).

Mutations in *CDKN2A* and *TP53* were only detected in MPNSTs and not in benign or atypical neurofibromas. The *CDKN2A* mutation (c.203dupC), found in LM1, leads to biallelic inactivation of *CDKN2A* in combination with a heterozygous deletion. This mutation has not previously been reported. In fact, tumor-specific *CDKN2A* mutations have not been described in NF1-related MPNSTs (Kourea et al., 1999; Nielsen et al., 1999). In contrast to *CDKN2A*, previous studies did report on *TP53* mutations in MPNSTs from NF1 patients. The percentage of MPNSTs harboring these mutations strongly differs among the various studies, which might be explained by the small sets of analyzed tumors (Verdijk et al., 2010). In our study, we observed three pathogenic *TP53* mutations in three high-grade MPNST cell lines, which were also listed in the "International Agency of Research on Cancer" *TP53* database. The fact that we did not find *TP53* mutations in tissue samples could be due to the heterogeneous nature of the tumors. In our tumor panel, *TP53* mutations were only detected in high-grade MPNSTs and not in low- or intermediate-grade. This can be explained by the fact that the number of samples analyzed was too low or by the hypothesis that mutations of

TP53 occur later on in tumor development. This is further confirmed by the fact that also *TP53* deletions are only seen in intermediate- and high-grade MPNSTs.

Clinically and genetically, we were not able to distinguish atypical neurofibromas from low-grade MPNSTs, but we only had two low-grade MPNSTs to compare with 16 atypical neurofibromas. Often both tumor types grow, cause pain and discomfort, with an increased glucose uptake on ^{18}F-FDG-PET scan. By aCGH and mutation analysis, we identified inactivation of *CDKN2A* as the recurrent lesion with the highest significance in both groups. On histology, an atypical neurofibroma is not the same as a low-grade MPNST. An atypical neurofibroma is characterized by a more variable cellularity than a benign neurofibroma and by cells with enlarged, hyperchromatic nuclei. MPNSTs were defined based on the WHO criteria and graded according to the French grading system, as stated in the "Materials and Methods" section. A low-grade MPNST is a uniformly hypercellular and fascicular lesion with generalized nuclear atypia. We histologically classified atypical neurofibromas and low-grade MPNSTs, but it is clear that there is still discussion about the use and definition of the terms atypical neurofibroma and low-grade MPNST (Weiss and Goldblum, 2008). This is not surprising, since it concerns lesions in the gray zone between benign and malignant, and the process of transformation is gradual.

The hypothesis that a benign neurofibroma undergoes malignant transformation toward MPNST through the stage of atypical neurofibroma is further confirmed by the fact that in some tumors, multiple regions with different histopathological features were seen. For example, in the tumor resected from patient 23, there was a transition from a benign outer part into an atypical deeper layer and further into the center consisting of intermediate-grade MPNST tissue (Fig. 2A). We were able to separate the outer layers (benign-atypical neurofibroma) from the internal MPNST tissue. We analyzed these samples by Agilent 244K aCGH analysis. The outer part (A7) showed a 9p21.3 deletion in a high percentage of cells and some other genetic imbalances in a lower amount of cells, consistent with an atypical neurofibroma. The inner nucleus (IM2) showed the same alterations as seen in A7, but in a larger proportion of cells, and a number of additional aberrations, as is typically seen in MPNSTs (Fig. 2B). The hypothesis was further confirmed by the fact that the same second hit was seen in both A7 and IM2, namely an identical type II *NF1* microdeletion (Fig. 2C). This is the first report describing the same somatic *NF1* mutation in samples with a different histology coming from the same tumor. The transition of a plexiform neurofibroma toward an MPNST through atypical neurofibroma was reported previously (Spurlock et al., 2010). Unfortunately, they were unable to prove that the different investigated tumor samples were part of the same tumoral lesion. The different samples were derived from separate nodules on the same peripheral nerve affected by NF1. This is in contrast to our data, where we clearly show that in one tumor we have a distinct transition from an outer part consisting of benign neurofibroma, a middle part of atypical neurofibroma, and a nucleus of intermediate-grade MPNST tissue, which is confirmed by both histopathological and molecular data.

In this report, several cell signaling pathways were found to play a role in the subsequent transformation and progression of MPNSTs. Receptor Tyrosine Kinase and Growth Factor Receptor pathways, namely the MAPK and PI3K pathways, are altered through amplification of *PDGFRA*, *KIT*, *EGFR*, and *MET* and deletion of *SPRY1*, *SPRY2*, and *PTEN*. Important cell cycle regulators such as *TP53*, *MDM2*, *CDKN2A/B/C*, *CDKN1C*, and *RB1* are also part of the recurrent copy number changes. Modifications in DNA repair gene *ATM*, apoptosis inhibitors (*BIRC5* and *TWIST1*), and neural crest transcription factors (*TWIST1* and *SOX9*) are part of the genetic events occurring during MPNST progression. Moreover, this study is the first report that links the development of MPNSTs to alterations in the chromatin remodeling genes *SUZ12*, part of the Polycomb Repressive Complex 2, and *SMARCA2/D1*, part of the SWI/SNF complex. This study highlights several significant recurrent copy number gains (12, 14q, 20q, and 21q) and losses (3q, 4q, 8p, 10, 13q, and 16q) that were not yet systematically linked to NF1-related MPNSTs. For most of these alterations, we proposed a number of genes potentially involved in the malignant transformation process. We cannot rule out that there are other rare copy number aberrations relevant for MPNST formation that were not statistically significant in our series.

We conclude that loss of the important cell cycle regulator, *CDKN2A*, is the hallmark of atypical neurofibromas. We showed that atypical neurofibromas should be considered as premalignant tumors.

ACKNOWLEDGMENTS

The authors thank Petra Weckx, Belinda Carleer, Christina Brusseleers, Marie-Josee Vanderheyden, and Julio Antonio Finalet Ferreiro for technical assistance.

REFERENCES

Birindelli S, Perrone F, Oggionni M, Lavarino C, Pasini B, Vergani B, Ranzani GN, Pierotti MA, Pilotti S. 2001. Rb and TP53 pathway alterations in sporadic and NF1-related malignant peripheral nerve sheath tumors. Lab Invest 81:833–844.

Brems H, Beert E, de Ravel T, Legius E. 2009. Mechanisms in the pathogenesis of malignant tumours in neurofibromatosis type 1. Lancet Oncol 10:508–515.

Cawthon RM, Weiss R, Xu GF, Viskochil D, Culver M, Stevens J, Robertson M, Dunn D, Gesteland R, O'Connell P, White R. 1990. A major segment of the neurofibromatosis type 1 gene: cDNA sequence, genomic structure, and point mutations. Cell 62:193–201.

De Raedt T, Brems H, Wolkenstein P, Vidaud D, Pilotti S, Perrone F, Mautner V, Frahm S, Sciot R, Legius E. 2003. Elevated risk for MPNST in NF1 microdeletion patients. Am J Hum Genet 72:1288–1292.

De Raedt T, Brems H, Lopez-Correa C, Vermeesch JR, Marynen P, Legius E. 2004. Genomic organization of the NF1 microdeletion region. Genomics 84:346–360.

Evans DG, Baser ME, McGaughran J, Sharif S, Howard E, Moran A. 2002. Malignant peripheral nerve sheath tumours in neurofibromatosis 1. J Med Genet 39:311–314.

Ferner RE, Golding JF, Smith M, Calonje E, Jan W, Sanjayanathan V, O'Doherty M. 2008. [18F]2-fluoro-2-deoxy-D-glucose positron emission tomography (FDG PET) as a diagnostic tool for neurofibromatosis 1 (NF1) associated malignant peripheral nerve sheath tumours (MPNSTs): A long term clinical study. Ann Oncol 19:390–394.

Glover TW, Stein CK, Legius E, Andersen LB, Brereton A, Johnson S. 1991. Molecular and cytogenetic analysis of tumors in von Recklinghausen neurofibromatosis. Genes Chromosomes Cancer 3:62–70.

Guillou L, Coindre JM, Bonichon F, Nguyen BB, Terrier P, Collin F, Vilain MO, Mandard AM, Le Doussal V, Leroux A, Jacquemier J, Duplay H, Sastre-Garau X, Costa J. 1997. Comparative study of the National Cancer Institute and French Federation of Cancer Centers Sarcoma Group grading systems in a population of 410 adult patients with soft tissue sarcoma. J Clin Oncol 15:350–362.

Holtkamp N, Okuducu AF, Mucha J, Afanasieva A, Hartmann C, Atallah I, Estevez-Schwarz L, Mawrin C, Friedrich RE, Mautner VF, von Deimling A. 2006. Mutation and expression of PDGFRA and KIT in malignant peripheral nerve sheath tumors, and its implications for imatinib sensitivity. Carcinogenesis 27:664–671.

Kehrer-Sawatzki H, Kluwe L, Sandig C, Kohn M, Wimmer K, Krammer U, Peyrl A, Jenne DE, Hansmann I, Mautner VF. 2004. High frequency mosaicism among patients with neurofibromatosis type 1 (NF1) with microdeletions caused by somatic recombination of the JJAZ1 gene. Am J Hum Genet 75:410–423.

Klijn C, Holstege H, de Ridder J, Liu X, Reinders M, Jonkers J, Wessels L. 2008. Identification of cancer genes using a statistical framework for multiexperiment analysis of nondiscretized array CGH data. Nucleic Acids Res 36:e13.

Kourea HP, Orlow I, Scheithauer BW, Cordon-Cardo C, Woodruff JM. 1999. Deletions of the INK4A gene occur in malignant peripheral nerve sheath tumors but not in neurofibromas. Am J Pathol 155:1855–1860.

Legius E, Marchuk DA, Collins FS, Glover TW. 1993. Somatic deletion of the neurofibromatosis type 1 gene in a neurofibrosarcoma supports a tumor suppressor gene hypothesis. Nat Genet 3:122–126.

Legius E, Dierick H, Wu R, Hall BK, Marynen P, Cassiman JJ, Glover TW. 1994. TP53 mutations are frequent in malignant NF1 tumors. Genes Chromosomes Cancer 10:250–255.

Lothe RA, Karhu R, Mandahl N, Mertens F, Saeter G, Heim S, Borresen-Dale AL, Kallioniemi OP. 1996. Gain of 17q24-qter detected by comparative genomic hybridization in malignant tumors from patients with von Recklinghausen's neurofibromatosis. Cancer Res 56:4778–4781.

Mantripragada KK, Spurlock G, Kluwe L, Chuzhanova N, Ferner RE, Frayling IM, Dumanski JP, Guha A, Mautner V, Upadhyaya M. 2008. High-resolution DNA copy number profiling of malignant peripheral nerve sheath tumors using targeted microarray-based comparative genomic hybridization. Clin Cancer Res 14:1015–1024.

Mantripragada KK, De Stahl TD, Patridge C, Menzel U, Andersson R, Chuzhanova N, Kluwe L, Guha A, Mautner V, Dumanski JP, Upadhyaya M. 2009. Genome-wide high-resolution analysis of copy number alterations in NF1-associated malignant peripheral nerve sheath tumors using the 32K BAC array. Genes Chromosomes Cancer 48:897–907.

Martin GA, Viskochil D, Bollag G, McCabe PC, Crosier WJ, Haubruck H, Conroy L, Clark R, O'Connell P, Cawthon RM, Innis MA, McCornick F. 1990. The GAP-related domain of the neurofibromatosis type 1 gene product interacts with ras p21. Cell 63:843–849.

Menon AG, Anderson KM, Riccardi VM, Chung RY, Whaley JM, Yandell DW, Farmer GE, Freiman RN, Lee JK, Li FP, Barker DF, Ledbetter DH, Kleider A, Martuza RL, Gusella JF, Seizinger BR. 1990. Chromosome 17p deletions and p53 gene mutations associated with the formation of malignant neurofibrosarcomas in von Recklinghausen neurofibromatosis. Proc Natl Acad Sci U S A 87:5435–5439.

Mertens F, Rydholm A, Bauer HF, Limon J, Nedoszytko B, Szadowska A, Willén H, Heim S, Mitelman F, Mandahl N. 1995. Cytogenetic findings in malignant peripheral nerve sheath tumors. Int J Cancer 61:793–798.

Mertens F, Dal Cin P, De Wever I, Fletcher CD, Mandahl N, Mitelman F, Rosai J, Rydholm A, Sciot R, Tallini G, van Den Berghe H, Vanni R, Willén H. 2000. Cytogenetic characterization of peripheral nerve sheath tumours: A report of the CHAMP study group. J Pathol 190:31–38.

Nielsen GP, Stemmer-Rachamimov AO, Ino Y, Moller MB, Rosenberg AE, Louis DN. 1999. Malignant transformation of neurofibromas in neurofibromatosis 1 is associated with CDKN2A/p16 inactivation. Am J Pathol 155:1879–1884.

Perrone F, Tabano S, Colombo F, Dagrada G, Birindelli S, Gronchi A, Colecchia M, Pierotti MA, Pilotti S. 2003. p15INK4b, p14ARF, and p16INK4a inactivation in sporadic and neurofibromatosis type 1-related malignant peripheral nerve sheath tumors. Clin Cancer Res 9:4132–4138.

Perry A, Kunz SN, Fuller CE, Banerjee R, Marley EF, Liapis H, Watson MA, Gutmann DH. 2002. Differential NF1, p16, and EGFR patterns by interphase cytogenetics (FISH) in malignant peripheral nerve sheath tumor (MPNST) and morphologically similar spindle cell neoplasm. J Neuropath Exp Neurol 61: 702–709.

Polito P, Dal Cin P, Debiec-Rychter M, Hagemeijer A. 2003. Human solid tumors: Cytogenetics techniques. In: Swansbury GJ, editor. Cancer Cytogenetics: Methods and Protocols. Totowa, NJ: Human Press, vol. 220, pp. 135–150.

Scheithauer BW, Woodruff JM, Erlandson RA, editors. 1999. Tumors of the peripheral nervous system. In: Atlas of Tumor Pathology, 3rd series. Fascicle 24. Washington, DC: Armed Forces Institute of Pathology, pp. 303–369.

Schmidt H, Taubert H, Meye A, Würl P, Bache M, Bartel F, Holzhausen HJ, Hinze R. 2000. Gains in chromosomes 7, 8q, 15q and 17q are characteristic changes in malignant but not in benign peripheral nerve sheath tumors from patients with Recklinghausen's disease. Cancer Lett 155: 181–190.

Schmidt H, Taubert H, Würl P, Bache M, Bartel F, Holzhausen HJ, Hinze R. 2001. Cytogenetic characterization of six malignant peripheral nerve sheath tumors: Comparison of karyotyping and comparative genomic hybridization. Cancer Genet Cytogenet 128:14–23.

Serra E, Rosenbaum T, Winner U, Aledo R, Ars E, Estivill X, Lenard HG, Lázaro C. 2000. Schwann cells harbor the somatic *NF1* mutation in neurofibromas: Evidence of two different Schwann cell subpopulations. Hum Mol Genet 9:3055–3064.

Spurlock G, Knight SJ, Thomas N, Kiehl TR, Guha A, Upadhyaya M. 2010. Molecular evolution of a neurofibroma to malignant peripheral nerve sheath tumor (MPNST) in an NF1 patient: Correlation between histopathological, clinical and molecular findings. J Cancer Res Clin Oncol 136:1869–1880.

Storlazzi CT, Brekke HR, Mandahl N, Brosjö O, Smeland S, Lothe RA, Mertens F. 2006. Identification of a novel amplicon at distal 17q containing the BIRC5/survivin gene in malignant peripheral nerve sheath tumours. J Pathol 209:492–500.

Trouche D, Le Chalony C, Muchardt C, Yaniv M, Kouzarides T. 1997. RB and hbrm cooperate to repress the activation functions of E2F1. Proc Natl Acad Sci U S A 94:11268–11273.

Veeriah S, Brennan C, Meng S, Singh B, Fagin JA, Solit DB, Paty PB, Rohle D, Vivanco I, Chmielecki J, Pao W, Ladanyi M, Gerald WL, Liau L, Cloughesy TC, Mischel PS, Sander C, Taylor B, Schultz N, Major J, Heguy A, Fang F, Mellinghoff IK, Chan TA. 2009. The tyrosine phosphatase PTPRD is a tumor suppressor that is frequently inactivated and mutated in glioblastoma and other human cancers. Proc Natl Acad Sci U S A 106:9435–9440.

Verdijk RM, den Bakker MA, Dubbink HJ, Hop WCJ, Dinjens WNM, Kros JM. 2010. TP53 mutation analysis of malignant peripheral nerve sheath tumors. J Neuropathol Exp Neurol 69:16–26.

Viskochil D, Buchberg AM, Xu G, Cawthon RM, Stevens J, Wolff RK, Culver M, Carey JC, Copeland NG, Jenkins NA, White R, O'Connell P. 1990. Deletions and a translocation interrupt a cloned gene at the neurofibromatosis type 1 locus. Cell 62:187–192.

Wallace MR, Marchuk DA, Andersen LB, Letcher R, Odeh HM, Saulino AM, Fountain JW, Brereton A, Nicholson J, Mitchell AL. 1990. Type 1 neurofibromatosis gene: Identification of a large transcript disrupted in three NF1 patients. Science 249:181–186.

Weiss SW, Goldblum RJ, editors. 2008. Soft Tissue Tumors: Benign Tumors of Peripheral Nerves. St Louis, MO: Mosby/Elsevier.